arXiv:cond-mat/0608068v3 [cond-mat.str-el] 4 Jun 2007

Charge and spin order on the triangular lattice — Na_xCoO_2 at $x = 0.5$

Sen Zhou and Ziqiang Wang
Department of Physics, Boston College, Chestnut Hill, MA 02467
(Dated: March 23, 2022)

The nature of electronic states due to strong correlation and geometric frustration on the triangular lattice is investigated in connection to the unconventional insulating state of Na_xCoO_2 at $x = 0.5$. We study an extended Hubbard model using a spatially unrestricted Gutzwiller approximation. We find a new class of charge and spin ordered states at $x = 1/3$ and $x = 0.5$ where antiferromagnetic (AF) frustration is alleviated via weak charge inhomogeneity. At $x = 0.5$, we show that the $\sqrt{3}a \times 2a$ off-plane Na dopant order induces weak $\sqrt{3}a \times 1a$ charge order in the Co layer. The symmetry breaking enables successive $\sqrt{3}a \times 1a$ AF and $2a \times 2a$ charge/spin ordering transitions at low temperatures. The Fermi surface is truncated by the $2a \times 2a$ hexagonal zone boundary into small electron and hole pockets. We study the phase structure and compare to recent experiments.

PACS numbers: 71.27.+a, 71.18.+y, 74.25.Jb, 74.70.-b

Sodium doped cobaltate Na_xCoO_2 has emerged recently as an important, layered triangular lattice fermion system with a rich phase structure [1]. These include a 5K superconducting phase near $x = 1/3$ upon hydration [2]; an A-type antiferromagnetic (AF) phase around $x = 0.8$ [3]; and an unexpected insulating state at $x = 0.5$ [1]. A series of experiments find the insulating state unconventional. While the magnetic susceptibility shows two cusps at $T_{m1} = 88$K and $T_{m2} = 53$K, the in-plane resistivity exhibits only a derivative feature at T_{m1}, followed by a metal-insulator transition below T_{m2} [1]. The insulating state has a small optical gap of 15meV [4, 5] and an anisotropic single-particle gap of ~ 8meV in angle resolved photoemission spectroscopy (ARPES) [6]. Electron diffraction [7, 8] shows that Na orders into $\sqrt{3}a \times 2a$ (hereafter we set $a = 1$) supercells below ~ 300K, suggesting that dopant order induced charge order may play a role in the insulating behaviors [1, 4, 9]. However, NMR experiments show that the Co valence exhibits small disproportionation with no appreciable change across the metal-insulator transition [10]. Bobroff et al. proposed that the insulating state is a result of successive SDW transitions due to the crossing of the Fermi surface (FS) with the orthorhombic zone boundary of $\sqrt{3} \times 2$ Na order [10]. Recently, elastic neutron scattering discovered that AF order occurs at T_{m1} with a 2×2 hexagonal unit cell [11]. The ordering vector is clearly incompatible with and challenges the SDW scenario.

In this paper, we study theoretically the electronic state at $x = 0.5$. The relevant low energy electronic structure involves three Co t_{2g} atomic orbitals forming one a_{1g} and two e'_g bands in the solid. In a recent work [17], starting from the three-band Hubbard model of the t_{2g} complex with LDA band dispersions [12], it is shown that strong correlation renormalizes the crystal field splitting and the bandwidths and drives the e'_g band below E_F, leaving a single band of mostly a_{1g} character near the Fermi level. The resulting quasiparticle dispersion and FS topology are in agreement with ARPES over a wide range of Na doping [13, 14, 15] as well as in hydrated samples [16]. This justifies a single-band model for the basic low energy physics, provided that the strong Coulomb repulsion is included at the Co site.

We consider here a single-band t-U-V model and study the interplay between the frustration of the kinetic energy and the AF spin correlations. Specifically, we extend the Gutzwiller approximation to the variational space spanned by spatially unrestricted and spin dependent densities. We find that the tendency towards inhomogeneity due to strong correlation and magnetic frustration work together to alleviate the AF frustration and produce a class of charge and spin ordered states. Hereafter, we use the terms inhomogeneity, charge and spin order interchangeably to refer to a nonuniform electronic state where the densities of charge and spin are spatially and periodically modulated. At $x = 1/3$, the ground state has spontaneous $\sqrt{3} \times \sqrt{3}$ charge and spin order even when $V = 0$. The frustration is avoided as the AF order develops on the honeycomb lattice and coexists with weak charge density modulations. At $x = 0.5$, we find that a large V is necessary to destabilize the uniform paramagnetic phase towards a state with $\sqrt{3} \times 1$ charge and AF spin order. This state is close to a Wigner crystal with a large charge disproportionation and a large insulating gap [18, 19], inconsistent with NMR [10], transport [1, 4, 5], and ARPES [6] experiments. We show that the $\sqrt{3} \times 2$ Na order at $x = 0.5$ induces a weak $\sqrt{3} \times 1$ charge order at high temperatures. The symmetry breaking allows $\sqrt{3} \times 1$ AF order to develop at T_{m1}. Remarkably, the FS at $x = 0.5$ coincides well with the 2×2 hexagonal zone boundary. This allows the 2×2 charge and spin order to develop by umklapp scattering at a lower temperature T_{m2}. The truncation of the FS into small electron and hole pockets marks the onset of the insulating behavior.

We begin with the one-band t-U-V model

$$H = \sum_{ij\sigma} t_{ij} c^\dagger_{i\sigma} c_{j\sigma} + U \sum_i \hat{n}_{i\uparrow} \hat{n}_{i\downarrow} + V \sum_{i>j} \frac{\hat{n}_i \hat{n}_j}{|\vec{r}_i - \vec{r}_j|}, \quad (1)$$

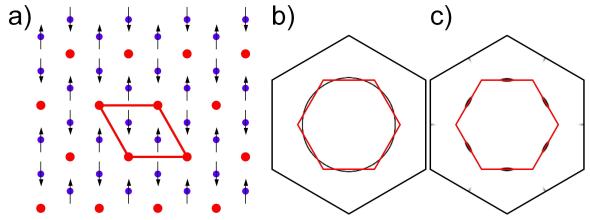


FIG. 1: (a) $\sqrt{3}\times\sqrt{3}$ charge and spin order at $x = 1/3$ and $V = 0$. The charge and spin densities are $x = (0.32, 0.36, 0.32)$ and $S^z = (0.18, 0.00, -0.18)$. (b) Nesting of $\sqrt{3}\times\sqrt{3}$ zone boundary with the paramagnetic FS. (c) Intensity of the quasiparticle peaks at the Fermi level.

where, $c^\dagger_{i\sigma}$ creates an a_{1g} *hole* of spin σ, $\hat{n}_i$ is the hole density operator, U and V are the on-site and long-range Coulomb repulsion. From the LDA a_{1g} band dispersion, the hopping parameters are chosen according to $t_{ij} = (-202, 35, 29)$meV for the first, second, and third nearest neighbors respectively. The local electron doping density is given by $x_i = 1 - n_i$. The large-U limit of Eq. (1) is usually treated in the Gutzwiller approximation (GA) [20, 21], which corresponds to the saddle point of the slave-boson path integral formulation [22]. Since the superexchange interaction is very small in the cobaltates due to the small bandwidth and large-U, we neglect the AF Heisenberg interaction [3] and consider magnetism of a kinetic origin. To encompass the Hilbert space with inhomogeneous charge/spin densities, we adopt a spatially unrestricted GA described by the renormalized mean-field Hamiltonian

$$H_{GA} = \sum_{ij\sigma} g^\sigma_{ij} t_{ij} c^\dagger_{i\sigma} c_{j\sigma} + \sum_{i,\sigma} \varepsilon_{i\sigma}(c^\dagger_{i\sigma} c_{i\sigma} - n_{i\sigma}) + V \sum_{i>j} \frac{\hat{n}_i \hat{n}_j}{|\vec{r}_i - \vec{r}_j|}, \quad (2)$$

where the Gutzwiller renormalization factor g^σ_{ij} depends on the sites connected by the hopping integral t_{ij},

$$g^\sigma_{ij} = \sqrt{\frac{x_i x_j}{(1-n_{i\sigma})(1-n_{j\sigma})}}. \quad (3)$$

The $\varepsilon_{i\sigma}$ in Eq. (2) is a spin dependent local fugacity that maintains the equilibrium condition and local densities upon Gutzwiller projection [23, 24]. It is determined by $\partial\langle H_{GA}\rangle/\partial n_{i\sigma} = 0$. The spin density is $S^z_i = (n_{i\uparrow} - n_{i\downarrow})/2$. If the charge density is forced to be uniform, the solution of Eq. (2) gives a stable paramagnetic phase up to $x_0 \simeq 0.67$ where a ferromagnetic (FM) transition takes place. The AF order, typical of large-U systems at small x on bipartite lattices [22], is absent due to geometrical frustration. We show below that this frustration can be alleviated by forming inhomogeneous electronic states.

To this end, we consider large triangular lattices of 240×320 sites with 6×8 unit cells wherein x_i, $n_{i\sigma}$, and $\varepsilon_{i\sigma}$ are allowed to have spatial variations. They are determined self-consistently by standard iterations. First let's consider the case at $x = 1/3$. It is remarkable that even for $V = 0$ the ground state has spontaneous $\sqrt{3}\times\sqrt{3}$ charge and spin order displayed in Fig. 1a. Frustration is alleviated as AF moments reside on the underlying unfrustrated honeycomb lattice. The tendency to avoid AF frustration is materialized because the FS at $x = 1/3$ coincides with the $\sqrt{3}\times\sqrt{3}$ zone boundary, as shown in Fig. 1b, such that *weak* charge order develops by the "umklapp" scattering and anisotropic gapping of the FS shown in Fig. 1c. We find that charge and spin sectors are coupled in the sense that the removal of inhomogeneity in either will reinstate the uniform paramagnetic phase. This state is thus different from the $\sqrt{3}\times\sqrt{3}$ charge ordered state proposed by Motrunich and Lee [25, 26] near $x = 1/3$, which is a Wigner crystal due to Coulomb jamming under a large V, involving no spin ordering and a large insulating gap. In contrast, our charge and spin ordered state has a very small insulating gap at $V = 0$ which increases gradually with increasing V. We point out that such a spin/charge ordered state has not yet been observed at $x = 1/3$, most likely because of the Na dopant disorder [27]. Indeed, we find that a disordered Na potential of moderate strength destroys the long-range order. It will be interesting to examine whether enhanced AF fluctuations in proximity to the ordered state can lead to superconductivity.

Next we turn to $x = 0.5$, which is not a natural commensurate filling on the triangular lattice. As a result, the uniform paramagnetic state is found to be stable for small $V < V_c$, $V_c \simeq 1.35$eV. For $V > V_c$, we find a first order transition to an inhomogeneous state with charge/spin order. Fig. 2 shows that, for $V = 1.5$eV, the moments are ordered into unfrustrated AF chains that are AF coupled and separated by nonmagnetic chains. This state is driven by strong long-range Coulomb V and stabilized by AF spin correlations. The charge density has a $\sqrt{3}\times 1$ unit cell with strong disproportionation close to the Co^{3+}/Co^{4+} configuration, resulting in a large charge gap. Indeed, similar "AF Wigner crystal" was recently proposed [19] and independently investigated by variational Monte Carlo on frustrated lattices [18]. It is important to note that while the $\sqrt{3}\times 1$ AF order can be described by a unit cell that is equivalent to the 2×2 hexagonal unit cell deduced from neutron scattering, the structure factor is different and the magnetic Bragg peaks shown in Fig. 2 (green squares) only has two-fold symmetry. This differs from the hexagonal Bragg peaks observed in neutron scattering, unless 120 degree orientated domains of equal contribution are present [11]. For this reason, we will continue to refer to this spin pattern as $\sqrt{3}\times 1$ AF order (see also Fig. 3b) and reserve the term 2×2 hexagonal unit cell for a state with hexagonal Bragg peaks (see Fig. 3c). In view of the experimental findings of weak charge disproportionation by NMR [10], and small insulating gaps by transport, optics, and ARPES [1, 4, 6], we conclude that this state, though indicative of the structure of the AF order by

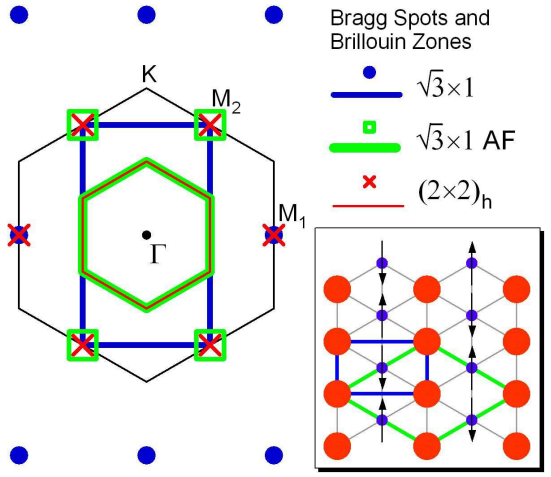


FIG. 2: $\sqrt{3}\times 1$ charge and AF spin order at $x = 0.5$ and $V = 1.5$eV (lower right). The charge and spin densities: $x = (0.05, 0.95, 0.05)$ and $S^z = (0.48, 0.00, -0.48)$. Also shown are charge and magnetic zones and Bragg peak locations of different structures. Note the absence of Bragg spot at M_1 for $\sqrt{3}\times 1$ AF order. $(2\times 2)_h$ corresponds to the hexagonal magnetic zone and Bragg spots of the state shown in Fig. 3c.

avoiding frustration via inhomogeneity, cannot describe the $x = 0.5$ phase of the cobaltates.

It turns out that the Na dopant order plays an important but subtle role at $x = 0.5$. Below about 300K, Na orders into $\sqrt{3}\times 2$ superlattice structures [7, 8]. This has led to the notion of an induced $\sqrt{3}\times 2$ electron charge order in the Co plane, which is ultimately responsible for the insulating state at $x = 0.5$. Three remarks are in order. First, the electrostatic potential from off-plane ordered ionic dopants in transition metal oxides is usually not strong due to screening by phonons, interband transitions, and the mobile carriers. Thus, the induced charge order in the basal plane is at most moderate. Second, as the temperature is lowered, FS stability may occur depending on the charge ordering symmetry. The latter can be different from the symmetry of dopant order. Due to the fact that the zigzag chains of ordered Na dopants above and below a Co layer are staggered, the superlattice potential felt by the electrons has a higher symmetry and results in $\sqrt{3}\times 1$ charge order with a much elongated orthorhombic zone than originally thought. Third, the breaking of the lattice symmetry makes it energetically favorable to develop AF order by alleviating frustration via weak charge inhomogeneity.

The effect of the Na dopant potential is to add

$$V_{\rm dopant}(i) = V_d \sum_{I=1}^{N_{\rm Na}} \frac{\hat{n}_i}{\sqrt{|\vec{r}_I - \vec{r}_i|^2 + d_z^2}} \qquad (4)$$

to Eq. (2), where V_d is the potential strength and $d_z \simeq a$ is the setback distance of Na to the Co plane. Including carrier screening of the dopant potential, we set $V = 0.2$eV and $V_d = 0.5$eV in the calculation. The Gutzwiller renormalized mean-field theory in Eq. (2) enables the calculation of the free-energy at finite temperatures. We present the temperature evolution of the self-consistently determined states in Fig. 3, and that of the charge and spin density in Fig. 4. At a temperature $k_BT = 20$meV above T_{m1}, marked in Fig. 4, the electronic state shown in Fig. 3a has $\sqrt{3}\times 1$ charge order induced by the Na potential *without* magnetic order. Note that the charge modulation shown in Fig. 4 is weak ($\sim 2\%$) and the FS in Fig. 3a is not affected. Lowering the intensity scale by four orders of magnitude reveals the weak band folding patterns along the intersections of the FS with the $\sqrt{3}\times 1$ zone boundary. As the temperature is reduced, we find an AF transition at T_{m1} marked in Fig. 4, below which $\sqrt{3}\times 1$ AF order develops and coexists with the $\sqrt{3}\times 1$ charge order. This state is shown in Fig. 3b at $k_BT = 14$meV. The transition is primarily a spin ordering transition, involving small changes in the charge disproportionation ($\sim 3\%$ from Fig. 4). This is consistent with NMR measurements [10]. Remarkably, Fig. 3b shows that the FS at $x = 0.5$ coincides well with the hexagonal magnetic zone boundary. However, since the structure factor of the $\sqrt{3}\times 1$ AF order breaks the hexagonal symmetry, the vertical sections of the FS remain intact as the scattering between them is switched off by the absence of the magnetic Bragg peak at M_1 in Fig. 2. Thermal broadening and the 120 degree domains may further weaken the features of T_{m1} in resistivity, op-

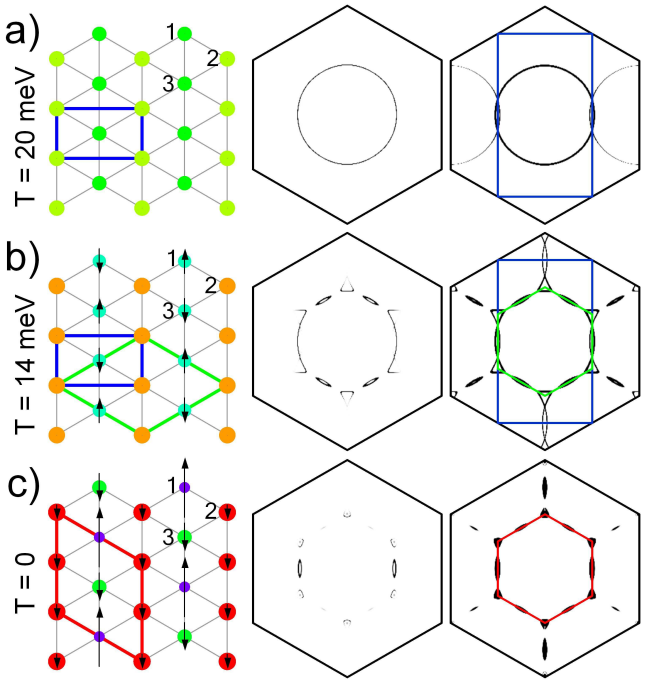


FIG. 3: The self-consistent states at $x = 0.5$ for three different temperatures (a), (b), and (c). First column: charge/spin ordering patterns and the unit cells. Second column: FS without thermal broadening showing the anisotropic gapping of the FS. Third column: FS when intensity scale is reduced by four orders of magnitude showing the band folding along zone boundaries of corresponding charge/spin order.

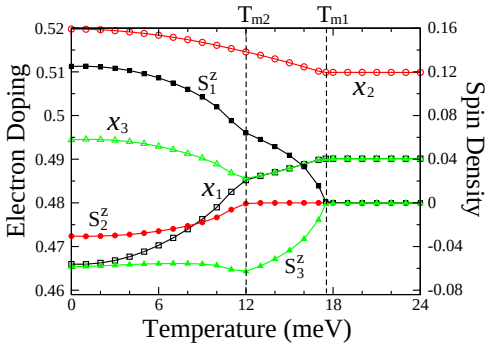


FIG. 4: Temperature evolution of charge (electron doping) and spin densities at three sites marked in Fig. 3. The spin/charge ordering transitions are marked by T_{m1} and T_{m2}.

tics, and ARPES measurements. Nevertheless, the FS topology change due to the emergence of electron-like FS pockets leads to the reduction and sign change in the Hall coefficient observed below T_{m1} [1].

Reducing the temperature further, we find a second transition marked as T_{m2} in Fig. 4 associated with additional symmetry breaking. Below T_{m2}, small magnetic moments develop at the Co(2) sites. They are coupled *ferromagnetically* as shown in Fig. 3c at $T = 0$. Below T_{m2}, the charge and spin densities in Fig. 4 are all different on the three inequivalent Co sites. Hence the ground state has charge and spin order with identical 2×2 hexagonal unit cell. Moreover, the Fourier transform of the spin density has now hexagonal Bragg peaks in a single domain (see Fig. 2) of similar weight at low temperatures. As a result of the combined 2×2 charge/spin order, the umklapp scattering destroys almost the entire FS as shown in Fig. 3c, leading to the onset of the metal-insulator transition below T_{m2}. The residual electron and hole-like FS pockets have six-fold symmetry with a two-fold anisotropy and provide an explanation for the existence of small FS pockets observed by Shubnikov-de Haas oscillations [28]. The low temperature insulating behavior develops by the localization of the electronic states on the small FS pockets, such that the insulating state has a nonzero density of states, and in this sense, a pseudogap. We emphasize that the most important character of the transition at T_{m2} is the emergence of small FM moments at Co(2). Its ordering direction should not be taken literally since it is specific to the restriction to collinear spins in the Gutzwiller approach. The FM moment on Co(2), collinear with the AF moments on Co(1) and Co(3), causes magnetic frustration and leads to an imbalance of the AF moments shown in Fig. 3c. In fact, it is more energetically favorable for the small FM moment to point orthogonal to the AF moment so as to avoid frustration of the in-plane AF order. The physics of the second transition is, however, unchanged. The small FM moments have been observed by NMR experiments [29, 30] as associated with the 53K transition, but they may be too small to have been detected in the neutron scattering experiments [11].

To summarize, we have shown that the unconventional insulating state at $x = 0.5$ is a result of the interplay among strong correlation, $\sqrt{3} \times 1$ weak charge order induced by Na dopant order, AF order by alleviated frustration, and the overlap of the FS with the 2×2 hexagonal magnetic zone boundary. A single band t-U-V model including the Na dopant potential for the electron doped, hole-like Co a_{1g} band on the triangular lattice captures the basic physics of the charge and spin order. The transition temperatures T_{m1} and T_{m2}, the size of the moments, and the insulating gap will depend on microscopic details and vary when Na is replaced by other isoelectronic atoms such as potassium in $K_{0.5}CoO_2$. However, the phase structure discussed here is expected to be universal of the cobaltate family at $x = 0.5$.

We thank H. Ding, Y. S. Lee, and especially P.A. Lee for many valuable discussions. This work is supported by DOE grant DE-FG02-99ER45747 and ACS grant 39498-AC5M.

[1] M.L. Foo et al., Phys. Rev. Lett. **92**, 247001 (2004).
[2] K. Takada, et. al., Nature (London) **422**, 53 (2003).
[3] S.P.Bayrakci et al., Phys. Rev. Lett. **94**, 157205 (2005).
[4] N.L. Wang et al., Phys. Rev. Lett. **93**, 147403 (2004).
[5] J. Hwang et al., Phys. Rev. B**72**, 024549 (2005).
[6] D. Qian et al., Phys. Rev. Lett. **96**, 046407 (2006).
[7] H.W. Zandbergen et al., Phys. Rev. B**70**, 024101 (2004).
[8] Q. Huang et al., J. Phys. Cond. Matt. **16**, 5803 (2004).
[9] K.-W. Lee et al., Phys. Rev. Lett. **94**, 026403 (2005).
[10] J. Bobroff et al., Phys. Rev. Lett. **96**, 107201 (2006).
[11] G. Gasparovic et al., Phys. Rev. Lett. **96**, 046403 (2006).
[12] D.J. Singh, Phys. Rev. B**61**, 13397 (2000).
[13] H.B. Yang et al., Phys. Rev. Lett. **95**, 146401 (2005).
[14] M.Z. Hasan et al., Phys. Rev. Lett. **92**, 246402 (2004).
[15] H.B. Yang et al., Phys. Rev. Lett. **92**, 246403 (2004).
[16] T. Shimojima et. al., cond-mat/0606424.
[17] S. Zhou et. al., Phys. Rev. Lett. **94**, 206401 (2005).
[18] H. Watanabe and M. Ogata, J. Phys. Soc. Jpn. **75**, 063702 (2006).
[19] T.P. Choy et. al., cond-mat/0502164.
[20] D. Vollhardt, Rev. Mod. Phys. **56**, 99 (1984).
[21] F.C. Zhang et al., Supercond. Sci. Techol. **1**, 36 (1998).
[22] G. Kotliar and A.E. Ruckenstein, Phys. Rev. Lett. **57**, 1362 (1986).
[23] C. Li et al., Phys. Rev. B**73**, 060501 (2006).
[24] Q.-H. Wang et al., Phys. Rev. B**73**, 092507 (2006).
[25] O.I. Motrunich and P.A. Lee, Phys. Rev. B**69**, 214516 (2004).
[26] H. Watanabe and M. Ogata, J. Phys. Soc. Jpn. **74**, 2901 (2005).
[27] D.J. Singh et. al., Phys. Rev. Lett. **97**, 016404 (2006).
[28] L. Balicas et al., Phys. Rev. Lett. **94**, 236402 (2005); *ibid*,Phys. Rev. Lett. **97**, 126401 (2006).
[29] T. Imai et al., cond-mat/0607625.
[30] M. Yokoi et. al., J. Phys. Soc. Jpn. **74**, 3046 (2005).